Mon. Not. R. Astron. Soc. **000**, 000–000 (0000) Printed 5 February 2008 (MN LATEX style file v1.4)

# On the black hole – bulge mass relation in active and inactive galaxies

R.J. McLure[1] & J.S. Dunlop[2]
[1] *Nuclear and Astrophysics Laboratory, University of Oxford, Keble Road, Oxford, OX1 3RH*
[2] *Institute for Astronomy, University of Edinburgh, Royal Observatory, Edinburgh EH9 3HJ.*



Accepted for publication in MNRAS

**ABSTRACT**
New black-hole mass estimates are presented for a sample of 72 AGN covering three decades in optical luminosity. Using a sub-sample of Seyfert galaxies, which have black-hole mass estimates from both reverberation mapping and stellar velocity dispersions, we investigate the geometry of the AGN broad-line region (BLR). It is demonstrated that a model in which the orbits of the line-emitting material have a flattened geometry is favoured over randomly orientated orbits. Using this model we investigate the $M_{bh}-L_{bulge}$ relation for a combined 90-object sample, consisting of the AGN plus a sample of 18 nearby inactive elliptical galaxies with dynamical black-hole mass measurements. It is found that, for all reasonable mass-to-light ratios, the $M_{bh}-L_{bulge}$ relation is equivalent to a linear scaling between bulge and black-hole mass. The best-fitting normalization of the $M_{bh}-M_{bulge}$ relation is found to be $M_{bh}=0.0012M_{bulge}$, in agreement with recent black-hole mass studies based on stellar velocity dispersions. Furthermore, the scatter around the $M_{bh}-L_{bulge}$ relation for the full sample is found to be significantly smaller than has been previously reported ($\Delta\log M_{bh}=0.39$ dex). Finally, using the nearby inactive elliptical galaxy sample alone, it is shown that the scatter in the $M_{bh}-L_{bulge}$ relation is only 0.33 dex, comparable to that of the $M_{bh}-\sigma$ relation. These results indicate that reliable black-hole mass estimates can be obtained for high redshift galaxies.

**Key words:** galaxies: active – galaxies: nuclei – galaxies:bulges – quasars: general

## 1 INTRODUCTION

The technique of using the broad H$\beta$ emission line to estimate the central black-hole masses of active galactic nuclei (AGN) has recently been employed widely in the literature (eg. Lacy et al. 2001, Laor 2001a, Wandel 1999). Given the ease with which the nuclear spectra of AGN can be obtained, a proper calibration of line-width black-hole mass estimates has the potential to allow the study of the evolution and demographics of active supermassive black holes over a wide range in redshift.

In a previous paper (McLure & Dunlop 2001, hereafter MD01) we reported H$\beta$ black-hole mass estimates for a 45-object sample consisting of both Seyfert galaxies and powerful ($M_V<-23$) quasars. By combining the black-hole mass estimates with host-galaxy bulge luminosities derived from full two-dimensional disc/bulge decompositions, MD01 found that quasars and Seyfert galaxies follow the same $M_{bh}-L_{bulge}$ relation, a result recently confirmed by Laor (2001a). Furthermore, by adopting a simple inclination correction factor for the H$\beta$ line widths, MD01 found that the mean $M_{bh}/M_{bulge}$ ratio in AGN is a factor of $2-4$ lower than had been determined by Magorrian et al. (1998) for nearby galaxies, in reasonable agreement with the results from recent stellar velocity dispersion studies (eg. Merritt & Ferrarese 2000a).

Despite the recent attention which has been focussed on determining the black-hole masses of both active and inactive galaxies, several important problems remain to be resolved, all of which are potentially soluble.

Firstly, at present the usefulness of the $M_{bh}-L_{bulge}$ relation as a black-hole mass estimator for both active and inactive galaxies is severely limited due to its large scatter ($\simeq 0.5$ dex). In our previous study (MD01) we demonstrated that much of this scatter could be due to the difficulty of accurately determining the bulge luminosities of late-type galaxies, even at $z<0.1$. Although the correlation between black-hole mass and stellar velocity dispersion for nearby inactive galaxies displays a much smaller scatter ($\simeq 0.3$ dex, Merritt & Ferrarese 2000b), it is still clear that a $M_{bh}-L_{bulge}$ correlation with reduced scatter would be highly desirable, given the extreme difficulty in obtaining

stellar velocity dispersions for high redshift galaxies. In this paper we investigate the possibility that the intrinsic scatter in the $M_{bh} - L_{bulge}$ relation is substantially lower than previously reported by studying a sample of nearby inactive galaxies for which $L_{bulge}$ has been determined to high accuracy.

A further complication which arises when studying the $M_{bh} - L_{bulge}$ relation for powerful active galaxies, is the uncertainty in how best to calibrate the virial black-hole mass estimates produced by using the broad H$\beta$ line-width to trace the central gravitational potential. Indeed, uncertainty about the exact geometry of the broad-line region (BLR) in AGN has the potential to produce large systematic errors in line-width based black-hole mass estimates (see Krolik 2000 for a discussion). In this paper we directly address this issue by adopting a flattened disc-like BLR geometry, which we demonstrate to be fully consistent with presently available data.

Thirdly, it is currently unclear whether the $M_{bh} - M_{bulge}$ relation is linear over a large baseline in bulge mass. Although our previous study (MD01) found no evidence for non-linearity in the $M_{bh} - M_{bulge}$ relation, the recent study of Laor (2001a) came to the opposite conclusion, finding that $M_{bh} \propto M_{bulge}^{1.54}$. As well as being of intrinsic interest, the question of the linearity of the $M_{bh} - M_{bulge}$ relation can also be used to constrain current models of combined black hole/bulge formation (eg. Kauffmann & Haehnelt 2000).

Fourthly, the results of our HST host-galaxy study (McLure et al. 1999, Dunlop et al. 2001) together with our previous H$\beta$ study (MD01), and the H$\beta$ study of Laor (2001b), point to an apparent division between the black-hole masses of optically selected radio-loud and radio-quiet quasars at $\simeq 10^9\,\mathrm{M}_\odot$. However, recent results from Lacy et al. (2001) and Dunlop et al. (2001) both indicate that this apparent threshold is not of fundamental physical importance. In this paper we use a large sample of 72 AGN, together with a sample of 20 nearby inactive galaxies with dynamic black-hole mass estimates, to systematically re-address these questions.

The structure of this paper is as follows. In Section 2 we describe the construction of the AGN and inactive galaxy samples. In Section 3 we briefly review the technique of estimating black-hole masses from emission-line widths, before proceeding to describe our adopted disc BLR model, and then to demonstrate that it is fully consistent with recent velocity dispersion measurements for a subset of our Seyfert galaxy sample. In Section 4 the normalization and linearity of the resulting $M_{bh} - L_{bulge}$ relation for the AGN and inactive galaxy samples is investigated and compared with literature results. In this section we also compare the $M_{bh} - L_{bulge}$ and $M_{bh} - \sigma$ relations for the inactive galaxy sample, and demonstrate that the scatter in both is virtually identical. In Section 5 we investigate the correlation between black-hole mass and the ratio of bolometric luminosity to the Eddington limit for the AGN sample. In Section 6 we explore the implications of the new black-hole mass estimates for the radio loudness dichotomy, before presenting our collusions in Section 7. To provide consistency with our previous study, all cosmological calculations in this paper assume $H_0 = 50$ $\mathrm{kms^{-1}Mpc^{-1}}$, $\Omega = 1.0$, $\Lambda = 0$.

| Sample | N | $L_{bulge}$ | H$\beta$ FWHM |
|---|---|---|---|
| QSO | 30 | MD01 | MD01 |
| QSO | 11 | H97 | F01 |
| QSO | 8 | MPD01 | BG92 |
| QSO | 4 | P01 | BG92 |
| Sy1 | 15 | MD01 | WPM99 |
| Sy1 | 4 | V00 | L01 |
| Inactive | 18 | F97 | - |

**Table 1.** Details of the data drawn from the literature. Column 2 lists the number of objects in each sub-sample. Column 3 lists the principle references for the bulge luminosity data. Column 4 lists the references for the H$\beta$ line-width data. The reference codes are as follows: MD01 (McLure & Dunlop 2001), H97 (Hooper et al. 1997), F01 (Forster et al. 2001), MPD01 (McLure, Percival & Dunlop 2001), BG92 (Boroson & Green 1992), P01 (Percival et al. 2001), WPM99 (Wandel, Peterson & Malkan 1999), V00 (Virani et al. 2000), L01 (Laor 2001a), F97 (Faber et al. 1997).

## 2 THE SAMPLE

The full sample analysed in this paper consists of 90 objects comprising three sub-samples of 53 quasars, 19 Seyfert 1 galaxies and 20 inactive nearby galaxies. This sample is a combination of the 45 objects from our previous study (MD01), together with 47 additional objects drawn from various literature sources. The principle objective behind the construction of the sample was to allow the study of the bulge: black-hole mass relationship over the widest possible dynamic range in both nuclear luminosity and central black-hole mass. Due to the fact that the sample is drawn from several sources, it was necessary to transform all the bulge luminosity data into the same filter. As in MD01, the chosen filter was the standard $R$-Cousins, which was preferred because measured $R-$band bulge luminosities were available for 65/72 of the AGN sample. The principle references for the bulge luminosity and line-width data are provided in Table 1, with specific details relating to each sub-sample provided below.

### 2.1 The quasar sample

The 53 objects in the quasar sample cover the redshift range $0.1 < z < 0.5$, and have absolute magnitudes ranging from $M_R \sim -22.5$ to $M_R \sim -28.0$. Consequently, the lowest luminosity quasars in the sample cover the overlap region around the Seyfert/quasar divide, while the highest luminosity objects constitute some of the most powerful quasars available at $z \leq 0.5$. Thirty of the objects are drawn from the quasar sample analysed in MD01, which have accurate $R-$band bulge luminosities from the host-galaxy study of Dunlop et al. (2001), and have line-width and optical continuum measurements from either our own recent observations (MD01), or the study of Boroson & Green (1992). The remaining 23 quasars in the new sample are drawn from three additional sources. Eleven further objects are taken from the HST host-galaxy study of LBQS quasars by Hooper et al (1997). The bulge luminosities are converted from the $R_J$ magnitudes published by Hooper et al. assuming $R_C - R_J = 0.1$ (Fukugita et al. 1995), with the line-width and continuum measurements taken from Forster et

al. (2001). Data for four objects is taken from the host-galaxy study of high-luminosity radio-quiet quasars by Percival et al. (2001). These quasars have $K-$band bulge luminosities based on sub-arcsecond tip/tilt imaging obtained at UKIRT, and optical spectra taken from Boroson & Green (1992). The final eight objects are taken from a new study (McLure, Percival & Dunlop 2001, in prep) of the host-galaxies of a radio-loud companion sample to that studied by Percival et al. The bulge luminosities in this study are taken from a combination of new $K-$band UKIRT observations and archive HST data. The optical spectra for these objects are also taken from Boroson & Green (1992). The bulge luminosities for those objects with $K-$band data were converted to the $R-$band assuming a rest-frame colour of $R-K=2.5$ (Dunlop et al. 2001).

### 2.2 The Seyfert galaxy sample

The Seyfert galaxy sample features the 15 objects analysed in MD01, with the addition of four objects from the Seyfert galaxy study of Virani et al. (2000) for which line-width data was available. In addition to the four new objects, the $R_C$ disc/bulge decompositions provided by Virani et al. have also been adopted for three objects from the MD01 sample (NGC 4051, NGC 4151, and NGC 3227). The bulge luminosities for these objects from Virani et al. replace those originally used by MD01, which were taken from Baggett, Baggett & Anderson (1998), and are preferred here because the data were obtained using the $R_C$ filter. The bulge luminosities for the other 12 objects remain the same as in MD01.

### 2.3 The inactive galaxy sample

The normal galaxy sample consists of eighteen objects drawn from the list of 37 nearby inactive galaxies with dynamical black-hole mass measurements published by Kormendy & Gebhardt (2001). Due to the difficulty in determining accurate bulge luminosities in late-type galaxies (see MD01 for a discussion) it was decided to exclude those galaxies in the Kormendy & Gebhardt list which were not of E-type morphology (including lenticulars). This decision was taken to investigate to what extent the scatter in the $M_{bh}-L_{bulge}$ relation could be reduced if the uncertainties in the bulge luminosities were minimized (see Section 4). The Kormendy & Gebhardt list consists of 20 E-type galaxies, which was reduced to the final 18-object sample by the exclusion of NGC 4486B and NGC 5845. These two objects were excluded because the errors on their black-hole mass measurements are an order of magnitude larger than for the rest of the sample (we note that NGC 4486B was also excluded as an outlier by Merritt & Ferrarese (2000b) in their study of black-hole demographics). The $B-$band bulge luminosities for 9 of the 18 objects were taken from Faber et al. (1997), with $V-$band data for a further 9 being taken from Merritt & Ferrarese (2000b). To convert the $B-$band and $V-$band magnitudes to the $R-$band, standard bulge colours of $B-R=1.57$ and $V-R=0.61$ were assumed (Fukugita et al. 1995). All eighteen objects in the sample have published velocity dispersion measurements, allowing a direct comparison of the $M_{bh}-L_{bulge}$ and $M_{bh}-\sigma$ relations (see Section 4).

## 3 THE VIRIAL BLACK-HOLE MASS ESTIMATE

The technique of using H$\beta$ line-widths to trace the gravitational potential of the central black holes which power AGN has been used extensively in recent years. Detailed discussions are provided by Wandel, Peterson & Malkan (1999) and Krolik (2001). The basic premise is that the dominant mechanism responsible for the width of the broad emission lines is the gravitational potential of the central black hole, and that the line-widths reflect the keplerian velocities of the line-emitting material (see Peterson & Wandel (2000) for supporting evidence). If this assumption is valid then the so-called virial mass estimate for the central black hole is given by:

$$M_{bh}=R_{BLR}V^2G^{-1} \quad (1)$$

where $R_{BLR}$ is the radius of the BLR and $V$ is the velocity of the line-emitting material. As in MD01, the method adopted in this paper for estimating the BLR radius is the correlation between $R_{BLR}$ and monochromatic luminosity at 5100Å found by Kaspi et al. (2000), from a combination of the reverberation mapping results for 17 PG quasars and 17 Seyfert galaxies (15 of which are in the sample studied here). Incorporating this into Eqn 1 yields the following formula for the black-hole mass:

$$M_{bh}=3.64\times f^2\times\left(\frac{\lambda L_{\lambda}(5100\text{Å})}{10^{37}W}\right)^{0.7}\times(FWHM)^2 \quad (2)$$

where $M_{bh}$ is the black-hole mass in solar units, FWHM is the full-width half maximum of the H$\beta$ line in kms$^{-1}$, and $f$ is a inclination factor which links the observed H$\beta$ FWHM to the intrinsic velocity of the line-emitting material. It can immediately be seen from Eqn 2 that the inclination factor $f$ can have a potentially large effect on the derived black-hole masses. Although evidence exists that radio-loud AGN display inclination dependent FWHMs consistent with a disc-like BLR (see below), in the radio-quiet population the geometry of the BLR is arguably undetermined. Consequently, the standard assumption made in the literature is that the velocities of the line-emitting material are randomly orientated, which leads to $f=\frac{\sqrt{3}}{2}$ (eg. Wandel 1999). However, as in our previous study (MD01), in this paper we adopt a specific model for the geometry of the broad-line region, which, as discussed below, is more consistent with the available data.

### 3.1 The disc model of the broad-line region

Following MD01 we make the assumption in this paper that the broad-line emitting material has a flattened disc-like geometry, and consequently that the observed H$\beta$ FWHM depends on the orientation of the disc rotation axis relative to the line of sight. Substantial evidence exists in the literature that the FWHM of broad emission lines are inclination dependent in radio-loud AGN (eg. Wills & Browne 1986, Brotherton 1996, Corbin 1997, Vestergaard, Wilkes & Barthel 2000). Such strong observational evidence does not exist for radio-quiet AGN, largely because the absence of radio jets removes one of the main methods with which to constrain the AGN orientation axis. However, the extension of a disc BLR model to the radio-quiet AGN in our

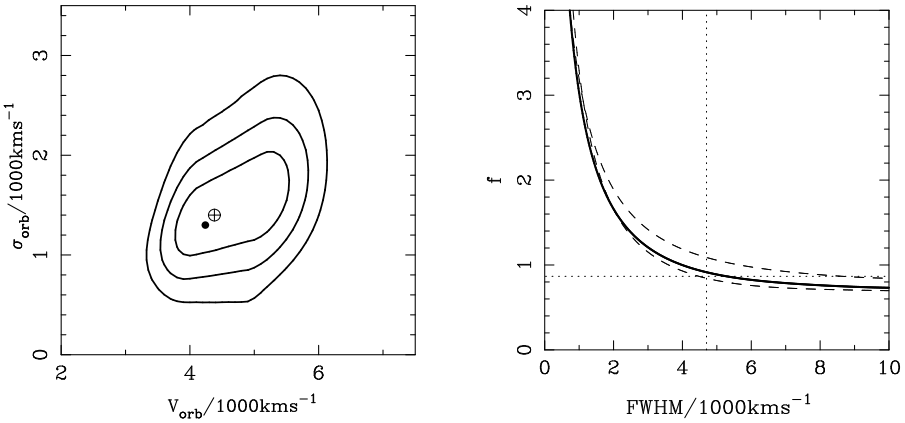


**Figure 1.** The left-hand panel shows the location (cross) of the best-fitting values of $V_{orb}$ and $\sigma_{orb}$, together with the $1, 2\,\&\,3\sigma$ joint confidence levels defined by $\Delta\chi^2 = 2.3, 6.2\,\&\,11.8$. Also shown (filled circle) is the location of the best-fitting parameters obtained by minimizing the Kolmogorov-Smirnov statistic between the model and data cumulative FWHM distributions. The right-hand panel shows the inclination correction factor ($f$) derived from the best-fitting parameters (solid line), together with the $\pm1\sigma$ models (dashed lines). Also shown is the effective inclination factor resulting from the assumption of random broad-line velocities (horizontal dotted line) and the mean observed FWHM of our sample (vertical dotted line).

sample can be justified on several grounds. Firstly, under the unified scheme (eg. Urry & Padovani 1995) it is expected that (to first order) the central engines, and presumably BLR, of radio-loud and radio-quiet AGN are essentially identical. Secondly, as will be discussed further below, previous studies have demonstrated that it is possible to fit the broad emission-line spectra of both radio-loud and radio-quiet AGN using a BLR model with a flattened geometry. Thirdly, as will be seen in Section 3.3, for those radio-quiet objects in our sample where it is possible to test the geometry of the BLR, it appears that the data are most consistent with a flattened geometry.

In order to determine the parameters of the chosen disc model we simply require that the model can reproduce the distribution of the observed H$\beta$ FWHMs. In MD01, the cumulative FWHM distribution of a smaller 45-object sample was fitted using a two-population model, where both subpopulations had the same characteristic orbital velocity, but were confined to lie within different ranges of inclination to the line of sight. Although the model adopted in MD01 provided an excellent fit to the available data, it was not fully satisfactory. The main reason for this is that because there was no way to individually allocate objects to one of the two populations, it was therefore only possible to calculate an average inclination correction, based on the sample as a whole. Consequently, it was therefore inevitable that objects with FWHM at the extremes of the observed distribution would not be properly corrected for inclination, systematically increasing the scatter in the resulting black-hole mass estimates.

Consequently, in the analysis of this new larger 72-object AGN sample it was decided to investigate the possibility of providing an acceptable description of the sample FWHM distribution using a single population model, uniquely determined by only three free parameters. This model makes the assumption that the intrinsic keplerian orbital velocities of the sample have a gaussian distribution, with mean $\bar{V}_{orb}$ and variance $\sigma^2_{orb}$. The third free parameter of the model is $\theta_{max}$, which is the maximum allowed angle between the line of sight and the disc rotation axis. In the model fit it is presumed that the angles between the line of sight and the disc rotation axis are randomly distributed between zero (pole-on) and $\theta_{max}$. In order to relate the intrinsic orbital velocities to the observed FWHMs we follow the results of the accretion disc modelling of Rokaki & Boisson (1999). Rokaki & Boisson used an accretion disc model to fit the UV continuum and H$\beta$ line profiles of a sample of 19 Seyfert 1 galaxies (9 of which are common to our sample) with the fitting process returning estimates of both central black-hole mass and the disc inclination angle. From their results for the 9 objects in common to both samples it follows that:

$$FWHM \simeq 2 \times sin(\theta)\,[GM_{bh}/R_{sat}]^{0.5} \quad (3)$$

where $R_{sat}$ is the radius at which the radial disc line-flux $F_l(r)$ saturates. It was shown by Rokaki & Boisson that the derived values of $R_{sat}$ are in good agreement with the broad-line radii $R_{BLR}$ derived from reverberation mapping observations. In this study we therefore make the assumption that $R_{BLR} = R_{sat}$, which immediately leads to $FWHM = 2V_{orb} \times sin(\theta)$. Consequently, in this disc model the inclination correction factor is simply $f = \frac{1}{2sin(\theta)}$.

### 3.2 Modelling the FWHM distribution

The parameters of the best-fitting model are determined by minimizing the chi-squared statistic between the model and data FWHM distributions. The best-fit parameter values ($\chi^2_{min} = 2.75, 5$ d.o.f.) determined from this process are as follows: $V_{orb} = 4375$ kms$^{-1}$, $\sigma_{orb} = 1400$ kms$^{-1}$ and $\theta_{max} = 47^{\circ}$. The location of the minimum chi-squared solution, together with the relevant confidence level contours, is shown in the left-hand panel of Fig 1. As a consistency check we have also determined the best-fit parameters by minimizing the Kolmogorov-Smirnov (KS) statistic between the model and data cumulative FWHM distributions. The location of this minimum is also indicated in Fig 1, and can be seen to be consistent with the minimum chi-squared so-

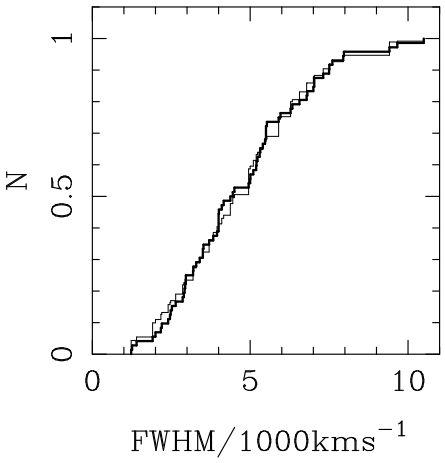


**Figure 2.** The cumulative FWHM distributions of the AGN sample (thick line) and the best-fitting disc BLR model (thin line). The two can be seen to be indistinguishable (KS, $p = 0.99$)

| Object | $\sigma$/kms$^{-1}$ | Reference |
|---|---|---|
| 3C 120 | 162 | NW95 |
| MRK 79 | 120 | F01 |
| MRK 590 | 169 | NW95 |
| MRK 817 | 140 | F01 |
| NGC 3227 | 128 | NW95 |
| NGC 3516 | 144 | A97 |
| NGC 4051 | 88 | NW95 |
| NGC 4151 | 85 | F01 |
| NGC 5548 | 180 | F01 |
| NGC 6814$\star$ | 115 | NW95 |

**Table 2.** The ten Seyfert galaxies in our sample which have published stellar velocity dispersions. All of the objects, with the exception of NGC 6814, also have reverberation mapping measurements of $R_{BLR}$. For NGC 6814 $R_{BLR}$ has been estimated from its continuum luminosity. Column three lists the literature sources for the velocity dispersions, with the following codes: NW95 (Nelson & Whittle 1995), F01 (Ferrarese et al. 2001) and A97 (Arribas et al. 1997).

lution. The quality of the model fit can be seen from Fig 2, which shows the cumulative FWHM distribution of the full 72-object sample and the best-fitting model. The application of the KS test confirms that the two distributions are essentially identical ($p = 0.99$).

The second panel of Fig 1 shows the inclination factor $f$ predicted by the best-fitting disc model, together with the predictions of the $\pm1\sigma$ models. Also shown in the plot (horizontal dashed line) is the effective inclination factor resulting from the assumption of randomly orientated BLR orbits; $f = \frac{\sqrt{3}}{2}$. The prediction of random orientated BLR orbits has been included to illustrate that the disc BLR model adopted here only makes significantly different predictions to the random case for those objects with observed FWHM$\leq$ 2800 kms$^{-1}$. For objects with FWHM$\geq$ 2800 kms$^{-1}$ (83% of the 72-object AGN sample) the inclination correction factor derived from our disc model differs by less than a factor of 2 from that resulting from the assumption of random velocities.

### 3.3 Testing the geometry of the broad-line region

Although the inclination corrections introduced by the disc BLR model only have a significant effect for a minority of objects in the AGN sample, it will be demonstrated in the next section that they significantly reduce the scatter in the $M_{bh} - L_{bulge}$ relation.

Due to this fact, it is important that the inclination dependence of the observed FWHM predicted by the disc BLR model can be shown to be at least consistent with the available data. As was discussed in Section 3.1, although there is substantial evidence in the literature for an inclination effect in the observed FWHM of radio-loud AGN, such evidence is not yet available for radio-quiet AGN. As a result, the justification for extending the disc model to radio-quiet objects relies primarily on the assumption that the central engine of all powerful AGN are essentially the same.

However, included in our 19-object Seyfert galaxy sample are 10 objects for which reliable stellar velocity dispersion measurements are available in the literature (see Table 2). Because stellar velocity dispersions are orientation independent, it follows that a direct comparison of the black-hole masses predicted by the $M_{bh} - \sigma$ relation with those of the orientation dependent H$\beta$ method will allow a test of the BLR geometry.

The procedure is as follows. For each of the ten Seyfert galaxies we first estimate their black-hole mass using the best-fitting $M_{bh} - \sigma$ relation to our nearby inactive galaxy sample (see Section 4) which has the form:

$$\log M_{bh} = 4.09(\pm0.58)\log(\sigma) - 1.26(\pm1.39) \quad (4)$$

and can be seen to be consistent with the $M_{bh} - \sigma$ relations determined by both Merritt & Ferrarese ($M_{bh} \propto \sigma^{4.72}$) and Gebhardt et al. (2000b)($M_{bh} \propto \sigma^{3.75}$). We then require for each object that this stellar velocity dispersion black-hole mass estimate be equal to the H$\beta$ virial black-hole mass estimate given by Eqn 1, using the reverberation mapping estimate of $R_{BLR}$ and assuming $V = f\times$FWHM. This provides a model-independent estimate of the inclination factor $f$ for each of the 10-objects. In Fig 3 we plot the estimated values of $f$ against observed FWHM for the ten Seyfert galaxies, along with the predicted curve from the disc BLR model, and the effective inclination factor resulting from the assumption of randomly orientated BLR velocities. From Fig 3 there can be seen to be good agreement between the derived inclination correction factors and those predicted by our adopted disc BLR model, particularly in the right-hand panel where the data have been binned. Also shown in the right-hand panel of Fig 3 is the inclination correction curve produced by fitting to the FWHM distribution of Seyfert galaxies alone. Due to its lower characteristic black-hole mass, it can be seen that this curve represents an improved match to the trend displayed by the binned data. We note here that the possible impact of fitting the various AGN sub-samples with different characteristic orbital velocities has been investigated. However, because the differences introduced into the black-hole mass estimates are small ($\sim 0.1$ dex), this more complicated procedure has negligible effect on the results presented in the rest of the paper. Consequently it was decided to adopt the best-fitting model to the full AGN sample throughout.

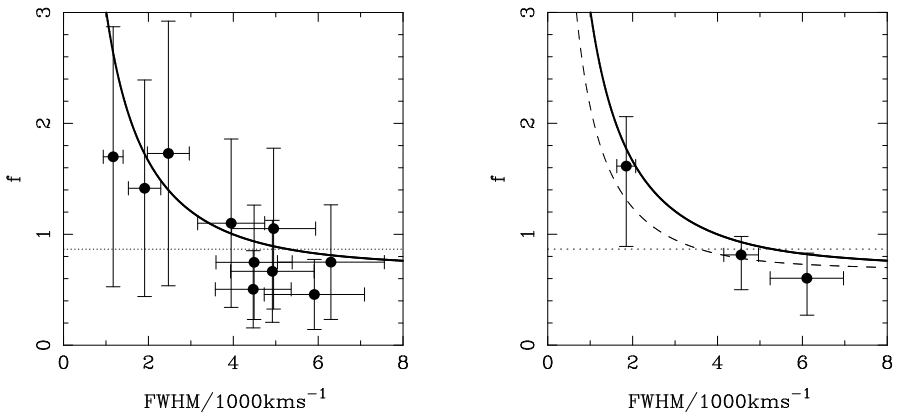


**Figure 3.** The left-hand panel shows the derived inclination factor ($f$) versus FWHM for the 10 Seyfert galaxies with measured stellar velocity dispersions (see text for discussion). Also shown is the prediction of the best-fitting disc BLR model to the full AGN sample (solid curve) and the expected value of $f$ in the case of purely random BLR velocities (dotted horizontal line). The error bars have been estimated by assuming a scatter of 0.3 dex in the $M_{bh} - \sigma$ relation and $\pm 15\%$ errors in FWHM measurements. The right-hand panel shows the same information using binning to clarify the trend displayed by the data. The dashed curve shows the inclination prediction of the best-fitting disc model to the complete $12\mu m$ Seyfert 1 sample of Rush, Malkan & Spinoglio (1993), which has a lower mean black-hole mass than our full AGN sample (see text for discussion).

Although the small sample size makes it unwise to draw any firm conclusions, we simply note that the assumption that the observed FWHM of the AGN sample are inclination dependent is at least consistent with the available data, and apparently more so than the assumption of purely random BLR velocities.

## 4 THE RELATIONSHIP BETWEEN BULGE LUMINOSITY AND BLACK-HOLE MASS.

In Fig 4 absolute $R-$band bulge magnitude is plotted against black-hole mass for the 72 objects in the AGN sample. Also shown is absolute $R-$band bulge magnitude plotted against dynamically-estimated black-hole mass for the 20 objects in our nearby inactive galaxy sample. Two aspects of Fig 4 are worthy of immediate comment. Firstly, as was shown by MD01 and Laor (1998 & 2001a), it can be seen that bulge luminosity and black-hole mass are extremely well correlated, with the Spearman rank correlation test returning $r_s = -0.77$ ($7.3\sigma$). Secondly, it is clear that the AGN and nearby inactive galaxy samples follow the same $M_{bh} - L_{bulge}$ relation over $> 3$ decades in black-hole mass, and $> 2.5$ decades in bulge luminosity. This second fact strongly supports the conclusions of Dunlop et al. (2001) and Wisotzki et al. (2001), that the host-galaxies of powerful quasars are normal massive ellipticals drawn from the bright end of the elliptical galaxy luminosity function. Thirdly, there can be seen to be no systematic offset between the Seyfert 1 and quasar samples, reinforcing the findings of MD01 and Laor (2001a) that, contrary to the results of Wandel (1999), the bulges of Seyfert galaxies and QSOs form a continuous sequence which ranges from $M_R$(bulge)$\simeq -18$ to $M_R$(bulge)$\simeq -24.5$. If we adopt an integrated value of $M_R^{\star} = -22.2$ (Lin et al. 1998), then this implies that the $M_{bh} - L_{bulge}$ relation holds from $L_{bulge} \simeq 0.01L^{\star}$, all the way up to objects which constitute some of the most massive ellipticals ever formed; $L_{bulge} \simeq 10L^{\star}$.

In order to find the best-fitting $M_{bh} - L_{bulge}$ relation we use the same iterative $\chi^2$ method used in MD01, which allows for measurement errors in both coordinates (Press et al. 1992). The best-fit to the full 90-object sample has the following form:

$$\log(M_{bh}/\,\mathrm{M}_{\odot}) = -0.50(\pm 0.02)M_R - 2.96(\pm 0.48) \qquad (5)$$

and is shown as the solid line in Fig 4. The scatter around this best-fitting relation is $\Delta M_{bh} = 0.39$ dex. It is worth noting that this level of scatter means that the $M_{bh} - L_{bulge}$ relation is now worthy of increased interest, given that it amounts to an uncertainty factor of $< 2.5$. Given that the 20 objects in the nearby inactive galaxy sample have actual dynamical black-hole mass estimates, it is obviously of interest to quantitatively test how consistent the $M_{bh} - L_{bulge}$ relation for these objects is with the fit to the full, AGN dominated, sample. The best-fit to the inactive galaxy subsample alone, has the following form:

$$\log(M_{bh}/\,\mathrm{M}_{\odot}) = -0.50(\pm 0.05)\mathrm{M_R} - 2.91(\pm 1.23) \qquad (6)$$

which can be seen to be perfectly consistent with the best-fit to the full sample in terms of both slope and normalization. Indeed, as shown in Table 3, the best-fitting relations for the full sample, quasar sample, Seyfert galaxy sample and the nearby inactive galaxy sample are all internally consistent, and display comparable levels of scatter. This is a remarkable result given that it implies that the combined bulge/black hole formation process was essentially the same throughout the full sample, which as well as featuring both active and inactive galaxies, includes galaxies of both late and early-type morphology.

The quality of the fit to the inactive galaxy sample is illustrated by the left-hand panel of Fig 5, which shows the $M_{bh} - L_{bulge}$ relation for the inactive galaxy sample alone. Of particular interest is the scatter around this best-fit relation, given that it has been widely reported in the literature (eg. Merritt & Ferrarese 2000b, Kormendy & Gebhardt 2001) that the scatter around the $M_{bh} - L_{bulge}$ relation is significantly greater than that around the $M_{bh} - \sigma$ rela-

| Sample | N | a | b | $\chi^2$ | $\Delta M_{bh}$ |
|---|---|---|---|---|---|
| All | 90 | $-2.96 \pm 0.48$ | $-0.50 \pm 0.02$ | 1.43 | 0.39 |
| Active | 72 | $-2.25 \pm 0.72$ | $-0.46 \pm 0.03$ | 0.94 | 0.42 |
| QSOs | 53 | $-4.26 \pm 3.15$ | $-0.55 \pm 0.13$ | 0.87 | 0.42 |
| Seyfert | 19 | $-1.96 \pm 1.33$ | $-0.45 \pm 0.06$ | 1.21 | 0.43 |
| Inactive | 20 | $-2.91 \pm 1.04$ | $-0.50 \pm 0.05$ | 1.05 | 0.33 |

**Table 3.** Details of the best-fitting relations of the form $\log M_{bh} = a + bM_R(bulge)$ to the full sample and to the various sub-samples. Column two gives the number of objects included in each fit. Columns three and four give the best-fitting values of the parameters $a$ & $b$, along with their associated uncertainties. The relatively large uncertainties in the fit to the QSO sub-sample reflects the small dynamic range in terms of both $L_{bulge}$ and $M_{bh}$. Column five gives the reduced $\chi^2$ for each fit and column 6 gives the scatter around each of the best-fitting relations in terms of $\Delta \log M_{bh}$.

tion. However, in contrast, we find that the scatter around the $M_{bh} - L_{bulge}$ relation for our sample of nearby inactive galaxies, which excludes non E-type morphologies, is only 0.33 dex, in excellent agreement with the scatter around the $M_{bh} - \sigma$ relation (Merritt & Ferrarese 2001b).

To test this result further, in the right-hand panel of Fig 5, we investigate $M_{bh} - \sigma$ relation for our nearby inactive galaxy sample. The scatter around the best-fit relation ($M_{bh} \propto \sigma^{4.09}$) is 0.30 dex, leading us to the conclusion that the intrinsic scatter around the $M_{bh} - L_{bulge}$ relation for elliptical galaxies is comparable to that in the $M_{bh} - \sigma$ relation. This may largely be due to the fact that when constructing the nearby inactive galaxy sample, objects with late-type morphologies were deliberately excluded. This would support the conclusion of MD01 that successful disc/bulge decomposition of late-type galaxies is a difficult task, even with high resolution data, and that bulge luminosities from ground-based images with poor seeing and, in particular, morphology-based estimates of bulge/total luminosity fraction (eg. Simien & de Vaucouleurs 1986) can often have substantial systematic errors associated with them. However, we also note that the late-type galaxies excluded from our nearby galaxy sample are not significant outliers with respect to the $M_{bh} - \sigma$ relation. Consequently, although our results indicate that bulge luminosity can provide accurate black-hole mass estimates, comparable with the $M_{bh} - \sigma$ relation, for elliptical galaxies, it is clear that the $M_{bh} - \sigma$ relation will provided more accurate black-hole mass estimates for samples which are not restricted to solely ellipticals.

### 4.1 The linearity of the bulge: black-hole mass relation

As pointed out in Section 1, one of the aims of this paper was to investigate the linearity of the $M_{bh} - M_{bulge}$ relation. In our previous study (MD01) of a sample of 45 AGN we found that $M_{bh} \propto M_{bulge}^{1.16 \pm 0.16}$, and therefore concluded that there was no evidence that the $M_{bh} - M_{bulge}$ relation was non-linear. In contrast, evidence for a non-linear relation was recently found by Laor (2001a). In his $V-$band study of the black hole to bulge mass relation in a 40-object sample

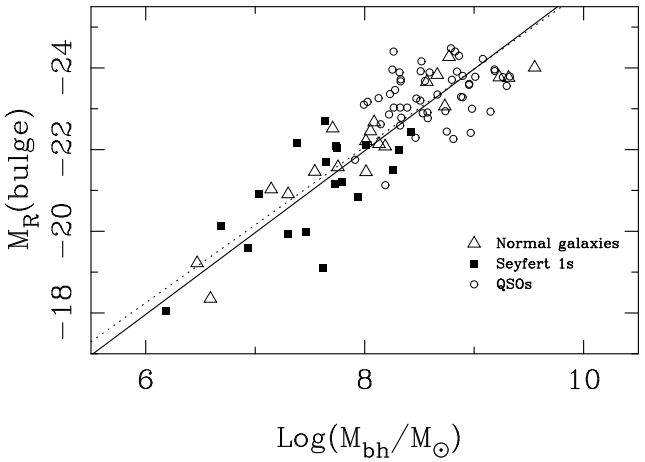


**Figure 4.** Absolute $R-$band bulge magnitude versus black-hole mass for the full 90-object sample. The black-hole masses for the 72 AGN are derived from their H$\beta$ line-widths under the disc-like BLR model. The black-hole masses of the inactive galaxies (triangles) are dynamical estimates as compiled by Kormendy & Gebhardt (2001). Also shown is the formal best-fit (solid line) and the best-fitting linear relation (dotted line).

(15 PG quasars, 16 inactive galaxies and 9 Seyfert galaxies) Laor found a best-fitting relation of the form:

$$M_{bh} = M_{bulge}^{1.54 \pm 0.15} \tag{7}$$

which is clearly apparently inconsistent with linearity. However, in order to determine the $M_{bh} - M_{bulge}$ relation it is obviously necessary to convert the measured bulge luminosities into masses, via an adopted mass-to-light ratio. The form of this mass-to-light ratio affects the derived slope of the $M_{bh} - M_{bulge}$ relation in the following way. If the mass-to-light ratio is parameterized as $M/L \propto L^{\alpha}$, then the resulting slope ($\gamma$) of the $M_{bh} - M_{bulge}$ relation is given by $\gamma = \frac{-2.5\beta}{1+\alpha}$, where $\beta$ is the slope of the $M_{bh} - L_{bulge}$ relation (Eqn 5).

As in MD01 we choose to adopt the derived $R-$band mass-to-light ratio for the Coma cluster from Jørgensen, Franx & Kjærgaard (1996), which has $\alpha = 0.31$. With this mass-to-light ratio the best-fitting $M_{bh} - L_{bulge}$ relation (Eqn 5) transforms to a $M_{bh} - M_{bulge}$ relation of the following form:

$$M_{bh} \propto M_{bulge}^{0.95 \pm 0.05} \tag{8}$$

It can immediately be seen that that there is no indication from our results that the relation is inconsistent with a linear scaling between black hole and bulge mass.

In order to calculate the bulge mass of the objects in his sample, Laor (2001a) adopted a $V-$band mass-to-light ratio of $M_{bulge} \propto L_{bulge}^{1.18}$ (Magorrian et al. 1998), which is significantly different from our chosen mass-to-light ratio. Indeed, if Laor (2001a) had adopted the mass-to-light ratio used here, then his best-fit to the $M_{bh} - M_{bulge}$ relation for his full sample would be $M_{bh} \propto M_{bulge}^{1.38 \pm 0.15}$, which is not formally inconsistent with linearity. However, irrespective of this, our new best-fit to the slope of the $M_{bh} - L_{bulge}$ relation ($\beta = -0.50 \pm 0.02$) of our new sample, which has a larger dynamic range in $L_{bulge}$ than both the samples studied in MD01 and Laor (2001a), means that any disagreement about mass-to-light ratios cannot now alter the conclusion

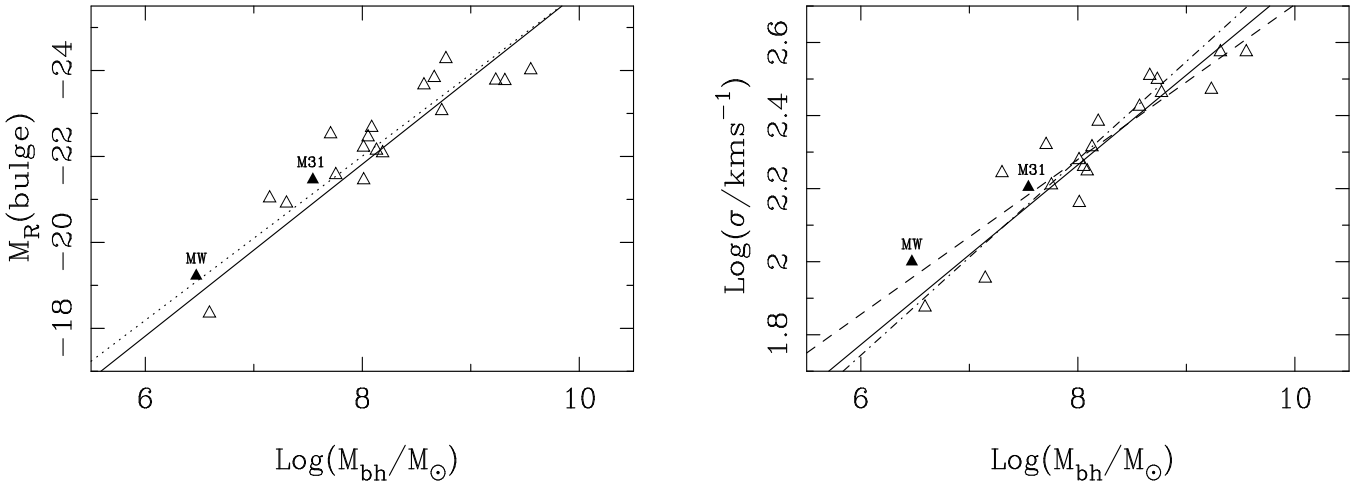


**Figure 5.** Left-hand panel shows absolute $R-$band bulge magnitude versus dynamical black-hole mass estimate for our 18-object inactive galaxy sample. The solid line is the best-fitting relation which has the form $M_{bh} \propto M_{bulge}^{0.95\pm0.09}$. The dotted line is the best-fitting linear relation to the full sample, and is equivalent to $M_{bh} = 0.0012 M_{bulge}$. The right-hand panel is the same with bulge luminosity replaced by stellar velocity dispersion. The solid line is the best-fit ($M_{bh} \propto \sigma^{4.09}$) , the dashed line is the Merritt & Ferrarese (2000b) relation ($M_{bh} \propto \sigma^{4.72}$), and the dot-dashed line is the Gebhardt et al. (2000b) relation ($M_{bh} \propto \sigma^{3.75}$). In both figures the location of the Milky Way and M31 are indicated for the interest of the reader, although neither was included in the nearby galaxy sample for the purposes of the analysis.

that the $M_{bh} - M_{bulge}$ relation is consistent with being linear. To demonstrate this we conclude by noting that even using the $M_{bulge} \propto L_{bulge}^{1.18}$ mass-to-light ratio adopted by Laor (2001a), our best-fitting $M_{bh} - L_{bulge}$ relation is equivalent to:

$$M_{bh} \propto M_{bulge}^{1.06\pm0.06} \quad (9)$$

again, completely consistent with a linear scaling.

### 4.2 The normalization of the $M_{bh} - M_{bulge}$ relation

Having established that the $M_{bh} - M_{bulge}$ relation is consistent with being linear, we now assume perfect linearity in order to establish the normalization of the $M_{bh} - M_{bulge}$ relation. With the mass-to-light ratio adopted here, a linear scaling corresponds to enforcing a slope of $-0.524$ in the $M_{bh}$ vs. $M_R$ relation. Under this restriction the best-fitting relation (dotted line in Figs 4 & 5a) has a normalization of $M_{bh} = 0.0012 M_{bulge}$, and can clearly be seen to be an excellent representation of the data. It is noteworthy that the normalization of $M_{bh} = 0.0012 M_{bulge}$ is identical to that determined by Merritt & Ferrarese (2000a) from their velocity dispersion study of the 32 inactive galaxies in the Magorrian et al. sample.

The closeness of the agreement between the $M_{bh}/M_{bulge}$ ratios determined here with those determined by Merritt & Ferrarese is highlighted by Fig 6, which shows a histogram of the $M_{bh}/M_{bulge}$ distribution for our 72-object AGN sample. The AGN $M_{bh}/M_{bulge}$ distribution has $\langle \log(M_{bh}/M_{bulge}) \rangle = -2.87 \pm 0.06$ with a standard deviation of $\sigma = 0.47$. This is in remarkably good agreement with the Merritt & Ferrarese results, which were $\langle \log(M_{bh}/M_{bulge}) \rangle = -2.90$ and $\sigma = 0.45$.

The close agreement between the distribution of $M_{bh}/M_{bulge}$ found here for the 72-object AGN sample and

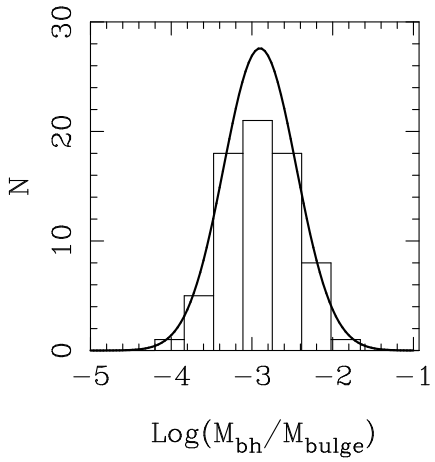


**Figure 6.** Histogram of the ratio of black-hole mass to bulge mass for the 72-object AGN sample. Over-plotted for comparison is a gaussian with $\langle \log(M_{bh}/M_{bulge}) \rangle = -2.90$ and standard deviation 0.45 (see text for discussion)

that found by Merritt & Ferrarese using velocity dispersions of nearby inactive galaxies, can also be taken as further supporting evidence that the adoption of a disc model for the BLR geometry is valid. Finally, we note that the normalization of $M_{bh} = 0.0012 M_{bulge}$ agrees very well with the predictions of recent models of coupled bulge/black hole formation at high redshift (Archibald et al. 2001).

## 5 THE BOLOMETRIC LUMINOSITY – BLACK-HOLE MASS CORRELATION

In this section we use the optical continuum information available for the AGN sample to investigate how bolometric luminosity as a fraction of the Eddington limit varies

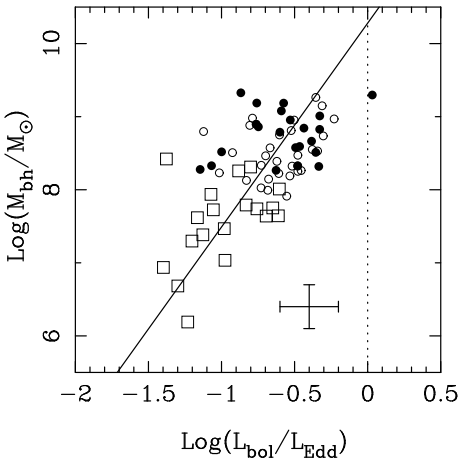


**Figure 7.** Black-hole mass plotted against bolometric luminosity as a fraction of the Eddington limit for the 72-object AGN sample. Radio-loud quasars are shown as filled circles, radio-quiet quasars are shown as open circles and the Seyfert galaxies are shown as open squares. The best-fitting relation is shown as the solid line, with the location of the Eddington limit shown by the vertical dotted line. Also shown is a representative error bar.

with black-hole mass. In order to estimate the bolometric luminosity of each AGN we follow Wandel, Peterson & Malkan (1998) and adopt $L_{bol} \simeq 10\lambda L_{5100}$, where $L_{5100}$ is the monochromatic luminosity at 5100 Å. Although this calibration was also found to be appropriate for the composite quasar spectrum of Laor et al. (1997), it is obviously only a rough estimate (Wandel, Peterson & Malkan 1998) and consequently we allow for a factor of 4 uncertainty when deriving the best-fitting relation.

In Fig 7 we plot black-hole mass against $L_{bol}/L_{Edd}$ for the full 72-object AGN sample. It can be seen that the two quantities are well correlated, with a Spearman rank coefficient of $r_s = 0.50, 4.2\sigma$. The best-fitting relation (solid line) has the following form:

$$\log M_{bh} = 2.79(\pm 0.37)\log(L_{bol}/L_{edd}) - 10.29(\pm 0.28) \quad (10)$$

and shows clearly that the data are inconsistent with all AGN having a constant Eddington ratio, a conclusion which was also arrived at by Kaspi et al. (2000). As in Fig 4, it is apparent that the Seyfert galaxies and quasars form a continuous sequence, and that in terms of Eddington ratio, there is no evidence for any systematic offset between the radio-loud and radio-quiet quasars. However, it is noteworthy that there is no evidence for a correlation within the QSO sub-sample alone. Indeed, given that the observed correlation is entirely dependent upon the heterogeneous Seyfert galaxy sample, it should perhaps be viewed with some caution. For example, it is inevitable that objects which should occupy the top-left corner of Fig 7 will be missing from our sample, since their large bulge luminosity and weak nuclear emission will have prevented them from being classified as powerful AGN. However, it is not immediately obvious why there should be no members of the Seyfert galaxy sample which are radiating at much closer to their Eddington limit. Although it is possible that the bottom-right of Fig 7 could be populated by so-called narrow-line Seyfert galaxies, which are thought to have intrinsically small black-hole masses and to radiate at a large fraction of their Eddington limit (eg. Mathur 2000), our present study does not support this. Four of the objects in the Seyfert galaxy sample have FWHM$\leq$ 2200 kms$^{-1}$ and yet do not occupy this region of the diagram. The implications of the $M_{bh} - L_{bol}/L_{Edd}$ relation, together with the $M_{bh} - M_{bulge}$ relation determined in the previous section, will be explored in a forthcoming paper (McLure, Percival & Dunlop, in prep).

## 6 BLACK-HOLE MASS AND THE RADIO-LOUDNESS DICHOTOMY

In this final section we investigate the relationship between black-hole mass and radio luminosity for the objects in the AGN sample, to explore the role played by black-hole mass in the quasar radio-loudness dichotomy. To ensure that any connection between black-hole mass and radio power can be investigated properly it is essential that the radio-quiet and radio-loud sub-samples should be indistinguishable in terms of both redshift and optical nuclear luminosity. From the total of 53 quasars in the AGN sample it has been possible to construct two sub-samples of radio-loud and radio-quiet quasars, numbering 23 and 26 objects respectively, which are well matched in term of redshift and optical luminosity ($\lambda L_{5100}$). The matching of the two sub-samples is confirmed by the application of the two-dimensional KS test (Peacock 1983), which returns a probability of $p = 0.25$ that the two distributions are indistinguishable in the $\lambda L_{5100} - z$ plane. Given that the quasars as a whole are a heterogeneous sample, this $\lambda L_{5100} - z$ matching is the best that can be done to ensure that any differences in the sub-sample black-hole mass distributions should be linked to the large differences in radio power.

The mean black-hole mass of the radio-quiet quasar sample is $\langle \log(M_{bh}/\mathrm{M}_\odot) \rangle = 8.61 \pm 0.07$, with a median value of $\log(M_{bh}/\mathrm{M}_\odot) = 8.56$. The black-hole masses of the radio-loud quasar sub-sample are somewhat larger on average, with a mean of $\langle \log(M_{bh}/\mathrm{M}_\odot) \rangle = 8.76 \pm 0.07$, and a median of $\log(M_{bh}/\mathrm{M}_\odot) = 8.83$. The suggestion from these results is that there does appear to be a tendency for the radio-loud quasars to have larger black-hole masses than their radio-quiet counterparts (the median figures differ by nearly a factor of 2), although the overlap between the two sub-samples is sufficient to ensure that the two black-hole mass distributions are not statistically distinguishable (KS, $p = 0.21$). Given that the radio-loud and radio-quiet sub-samples were deliberately chosen to be matched in terms of their nuclear optical luminosity, it is clear from Eqn 2 that the difference in average black-hole mass between the two sub-samples must be due to differences in observed H$\beta$ FWHM. This does appear to be the case, and can be seen in Fig 8, which shows a plot of optical luminosity against observed FWHM for the two sub-samples. As is highlighted in Fig 8 there is a separation around FWHM=5500 kms$^{-1}$, with 11/23 RLQs having FWHM $>$ 5500 kms$^{-1}$, while only 4/26 RQQs have FWHM$>$ 5500 kms$^{-1}$. This difference is confirmed as being significant, with the KS test returning a probability of $p = 0.05$ that the two FWHM distributions are drawn from the same parent distribution. The difference in the FWHM distributions between radio-loud and radio-quiet quasars has been previously reported at higher signif-

icance ($p = 0.001$) from the larger-scale spectrophotometric studies of Corbin (1997) and Boroson & Green (1992).

The suggestion that the black holes of radio-loud quasars are on average more massive than their radio-quiet counterparts is consistent with the results of our recent host-galaxy study (Dunlop et al. 2001, McLure et al. 1999), our previous H$\beta$ line-width study (MD01) and the recent line-width study of the LBQS by Laor (2001b). In this study, Laor calculated virial black-hole mass estimates for the 87 LBQS objects with $z < 0.5$, finding an apparent separation between the radio-loud and radio-quiet quasars at a black-hole mass of $\simeq 10^9\,\mathrm{M}_\odot$. However, it is important to remember that the radio-loud objects in both of these studies are predominantly optically selected. The possible weakness of using optically selected quasar samples to study the link between black-hole mass and radio power has recently been highlighted by Lacy et al. (2001). In their line-width study of a virtually complete sub-sample of the FBQS, Lacy et al. find that the apparent gap in the radio: black-hole mass plane is filled in by radio intermediate quasars, and that the quasar population as a whole follows a relation of the form: $P_{5GHz} \propto M_{bh}^{1.9}(L/L_{edd})^{1.0}$.

Although the black-hole masses and 5GHz radio luminosities of the radio-loud quasars analysed here are consistent with the results of Lacy et al., the large scatter around the Lacy et al. relation (1.1 dex) makes this somewhat inevitable. In fact, we argue elsewhere (Dunlop et al. (2001), McLure & Dunlop, in prep) that the data are more consistent with the existence of an upper and lower envelope to the radio power that can be produced by a black hole of a given mass. Consequently, we argue that in order to produce a truly radio-loud AGN ($P_{5GHz} \simeq 10^{25}$ WHz$^{-1}$sr$^{-1}$), the central black-hole mass must be $\geq 10^{8.5}\,\mathrm{M}_\odot$ and lie on the upper $M_{bh} - P_{5GHz}$ envelope (see Dunlop et al. (2001) for a full discussion). Finally, we note that this picture of the radio-loudness dichotomy is in good agreement with the predictions of the merger model proposed by Wilson & Colbert (1995), in which the radio-loudness of an AGN is dependent on both the mass and angular momentum of the central black hole.

## 7 CONCLUSIONS

New virial black-hole mass estimates have been presented for a sample of 72 AGN using the FWHM of the broad H$\beta$ emission line, corrected for inclination under the assumption of a disc-like broad-line region. The form of the $M_{bh} - M_{bulge}$ relation is investigated using reliable bulge luminosity measurements for both the AGN sample and a carefully selected sample of nearby inactive galaxies with dynamical black-hole mass measurements. Using the inactive nearby galaxy sample a rigorous comparison was made of the scatter around the $M_{bh} - L_{bulge}$ and $M_{bh} - \sigma$ relations. The main conclusions of this study can be summarized as follows:

- For a 10-object subset of the Seyfert galaxy sample it is found that the inclination predictions of a disc model BLR are more consistent with the available data than the assumption of purely random broad-line velocities.
- A strong correlation ($7.3\sigma$) is found between bulge luminosity and black-hole mass estimated via the disc BLR model.

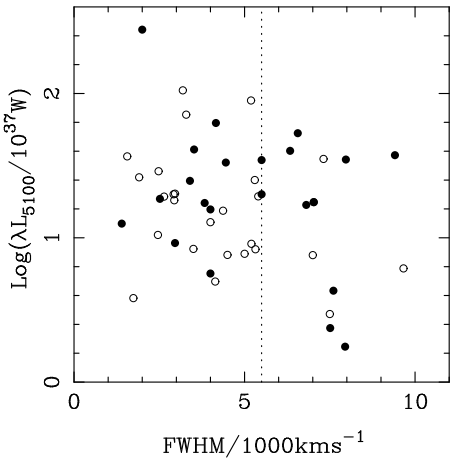


**Figure 8.** The distribution of the radio-loud and radio-quiet quasar sub-samples in the $\lambda L_{5100} - $FWHM plane. It should be noted that there is a significant difference in the FWHM distributions of the two samples (KS, $p = 0.05$), with 11/23 radio-loud quasars having FWHM$> 5500$ kms$^{-1}$ while only 4/26 radio-quiet quasars have FWHM$> 5500$ kms$^{-1}$.

- The best-fitting $M_{bh} - L_{bulge}$ relation to the combined sample of 72 AGN and 18 nearby inactive elliptical galaxies is found to be consistent with a linear scaling between black hole and bulge mass ($M_{bh} \propto M_{bulge}^{0.95\pm0.05}$), and to have much lower scatter than previously reported ($\Delta \log M_{bh} = 0.39$ dex).
- The best-fitting normalization of the $M_{bh} - M_{bulge}$ relation is found to be $M_{bh} = 0.0012 M_{bulge}$, in excellent agreement with recent stellar velocity dispersion studies.
- In contrast to previous reports it is found that the scatter around the $M_{bh} - L_{bulge}$ and $M_{bh} - \sigma$ relations for the nearby inactive elliptical galaxy sample are comparable, at only $\sim 0.3$ dex.
- Using samples matched in terms of optical luminosity, the median black-hole mass of radio-loud quasars is found to be larger by 0.27 dex than that of their radio-quiet counterparts. This difference is found to be due to a small but significant ($p = 0.05$) difference in their respective FWHM distributions.

## 8 ACKNOWLEDGMENTS

The United Kingdom Infrared Telescope is operated by the Joint Astronomy Centre on behalf of the U.K. Particle Physics and Astronomy Research Council. Based on observations with the NASA/ESA Hubble Space Telescope, obtained at the Space Telescope Science Institute, which is operated by the Association of Universities for Research in Astronomy, Inc. under NASA contract No. NAS5-26555. This research has made use of the NASA/IPAC Extragalactic Database (NED) which is operated by the Jet Propulsion Laboratory, California Institute of Technology, under contract with the National Aeronautics and Space Administration. RJM acknowledges the award of a PPARC postdoctoral fellowship. JSD acknowledges the enhanced research time afforded by the award of a PPARC senior research fellowship.

## REFERENCES


Archibald E.N., Dunlop J.S., Jimenez R., Friaca A.C.S., McLure R.J., Hughes D.H., 2001, MNRAS, submitted, astro-ph/0108122

Arribas S., Mediavilla E., Garćia-Lorenzo B., Del Burgo C., 1997, ApJ, 490, 227

Baggett W.E., Baggett S.M., Anderson K.S.J., 1998, AJ, 116, 1626

Boroson T.A., Green R.F., 1992, ApJS, 80,109

Brotherton M.S., ApJS, 1996, 102, 1

Corbin M.R., 1997, ApJS, 113, 245

Dunlop J.S., McLure R.J., Kukula M.J., Baum S.A., O'Dea C.P., Hughes D.H., 2001, MNRAS, submitted, astro-ph/0108397

Faber et al., 1997, AJ, 114, 1771

Forster K., Green P.J, Aldcroft T.L., Vestergaard M., Foltz C.B., Hewett P.C., 2001, ApJS, 134, 35

Ferrarese L., Pogge R.W., Peterson B.M., Merritt D., Wandel A., Joseph C.L., 2001, ApJ, 555, L79

Franceschini A., Vercellone S., Fabian A.C., 1998, MNRAS, 297, 817

Fukugita M., Shimasaku K., Ichikawa T., 1995, PASP, 107, 945

Gebhardt K., et al., 2000b, ApJ, 539, L13

Gebhardt K., et al., 2000a, ApJ, 543, L5

Hooper E.J., Impey C.D., Foltz C.B., 1997, ApJ, 480, L95

Jørgensen I., Franx M., Kjærgaard P., 1996, MNRAS, 280, 167

Kaspi S., Smith P.S., Netzer H., Maoz D., Jannuzi B.T., Giveon U., 2000, ApJ, 533, 631

Kauffmann G., Haehnelt M., 2000, MNRAS, 311, 576

Kormendy J., Gebhardt K., 2001, astro-ph/0105230

Krolik J.H., 2001, ApJ, 551, 72

Lacy M., Laurent-Muehleisen S.A., Ridgway S.E., Becker R.H., White R.L., 2001, ApJ, 551, L17

Laor A., 1998, ApJ, 505, L83

Laor A., 2001b, ApJ, 543, L111

Laor A., 2001a, ApJ, 553, 677

Lin H., Kirshner P.P., Schectman S.A., Landy S.D., Oemler A., Tucker

McLure R.J., Dunlop J.S., Kukula M.J., Baum S.A., O'Dea C.P., Hughes D.H., 1999, MNRAS, 308, 377

McLure R.J., Dunlop J.S., 2001, MNRAS, in press, astro-ph/0009406

Magorrian J., et al., 1998, AJ, 115, 2285

Mathur S., 2000, MNRAS, 314, L17

Merritt D., Ferrarese L., 2001a, MNRAS, 320, L30

Merritt D., Ferrarese L., 2001b, ApJ, 547, 140

Nelson C.H., Whittle M., 1995, ApJS, 99, 67

Peacock J.A., 1983, MNRAS, 202, 615

Percival W.J., Miller L., McLure R.J., Dunlop J.S., 2001, MNRAS, 322, 843

Peterson B.M., Wandel A., ApJ, 2000, 540, L13

Press W.H., Teukolsky S.A., Vetterling W.T., Flannery B.P., 1992, Numerical Recipes, Cambridge University Press

Rokaki E., Boisson C., 1999, MNRAS, 307, 41

Rush B., Malkan M., Spinoglio L., 1993, ApJS, 89, 1

Simien F., de Vaucouleurs G., 1986, ApJ, 302, 564

Urry M., Padovani P., 1995, PASP, 107, 803

Véron-Cetty, M.P.; Véron, P., 2001, A&A, 374, 92

Vestergaard M., Wilkes B.J., Barthel P.D., 2000, ApJ, L103

Virani S.N., De Robertis M., VanDalfsen M.L., 2000,AJ, 120, 1739

Wandel A., 1999, ApJ, 519, L39

Wandel A., Peterson B.M., Malkan M.A., 1999, ApJ, 526,579

Wills B.J., Browne I.W.A., 1986, ApJ, 302, 56

Wilson A.S., Colbert E.J.M., 1995, ApJ, 438, 62

Wisotzki L., Kuhlbrodt B., Jahnke K., astro-ph/0103112